ELSEVIER

Soil Dynamics and Earthquake Engineering 27 (2007) 703–711

SOIL DYNAMICS AND EARTHQUAKE ENGINEERING

www.elsevier.com/locate/soildyn

Wave-passage effects on strength-reduction factors for design of structures near earthquake faults

R.S. Jalali[a], M.D. Trifunac[b,*], G. Ghodrati Amiri[c], M. Zahedi[a]

[a]*Department of Civil Engineering, Iran University of Science and Technology, Narmak, Tehran 16846, Iran*
[b]*Department of Civil Engineering, University of Southern California, Los Angeles, CA 90089, USA*
[c]*Center of Excellence for Fundamental Studies in Structural Engineering, Department of Civil Engineering, Iran University of Science and Technology, Narmak, Tehran 16846, Iran*

Received 13 September 2006; received in revised form 12 January 2007; accepted 28 January 2007

Abstract

Wave-passage effects are described for strength-reduction factors near faults, for fault-normal and fault-parallel strong-motion displacements. It is shown that the common design rules for selection of the strength-reduction factors are usually conservative and approximately describe the reduction amplitudes near faults of strong earthquakes for fault-normal pulses. However, for fault-parallel displacements, the same reduction factors are not conservative and must be changed. It is recommended that for design close to active faults, the strength-reduction factors for all components of motion should be constant for long periods and equal to $(2\mu-1)^{1/2}$, where μ is ductility. For periods shorter than about 1 s, these strength reduction factors should be further reduced by 30–40%.

Keywords: Strength-reduction factors; Differential motions; Non-linear response; Near field; Earthquake motion; Design of structures

1. Introduction

For many design analyses, the earthquake shaking can be specified at a single point, and the spatial variation of motion at multiple supports of structures may be neglected. When the distances between the multiple support points are large (e.g., bridges, dams, tunnels, long buildings), the effects of differential motions become important and should be considered in dynamic analyses [1]. Spatial and temporal stochastic representations of strong earthquake motion required for such analyses have been investigated [2–4]. The consequences of differential ground motion have been studied for the response of beams [5–7], bridges [8–10], simple models of three-dimensional structures [11], long buildings [12–15] and dams [16–18]. However, with few exceptions, engineering applications of the response spectrum method ignore the wave-propagation effects in the foundation soil, or they consider only a simplified stochastic representation of the differences in motion among separate supports [19–21]. Okubo et al. [22] were among the first to measure and interpret finite ground strains of recorded earthquake motions for plan dimensions representative of intermediate and large buildings. They showed that for short-period (stiff) structures, finite ground strains lead to increased base shears. Zembaty and Krenk [23,24] studied the same model via random vibration-based shear force response spectrum, addressing explicitly the contribution of quasi-static and dynamic terms in the response. They showed that although the relative response of the structure is reduced in the case of differential motion of supports (due to "averaging" of spatially correlated motions), the shear forces in the columns, which for stiff structures primarily depend upon the quasi-static contribution to the response, might be significantly larger than for synchronous excitation.

Simple analyses of two-dimensional models of long buildings suggest that when $a/\lambda < 10^{-4}$, where a is wave amplitude and λ is the corresponding wavelength, the wave-propagation effects on the response of simple structures can be neglected [14]. For shorter waves, but

*Corresponding author. Tel.: +1 231 740 0570; fax: +1 231 744 1426.
E-mail addresses: saleh@iust.ac.ir (R.S. Jalali), trifunac@usc.edu (M.D. Trifunac).

0267-7261/$ - see front matter © 2007 Elsevier Ltd. All rights reserved.
doi:10.1016/j.soildyn.2007.01.006

those still longer than the characteristic dimensions of the structure, Trifunac and Gicev [25] and Trifunac and Todorovska [26] showed that the common response spectrum method for synchronous ground motion can be extended to make it applicable for earthquake response analyses of extended structures experiencing differential in-plane and out-of-plane ground motion.

In the engineering design of earthquake-resistant structures by pushover analyses [27–29], the design is governed by target displacements determined from the inelastic response of the corresponding single-degree-of-freedom system (SDOF). For estimation of the maximum nonlinear response of an SDOF system, u_m, in terms of the maximum linear response, u_0, it is necessary to specify a relation between u_m and u_0. By defining the yield strength reduction factor as $R_y = u_0/u_y$, where u_y is the yielding displacement of the SDOF system equivalent spring, and ductility as $\mu = u_m/u_y$, for the same ground motion, the ratio u_m/u_0 is then equal to μ/R_y. The relationship between u_m and u_0 (Fig. 1a) for the same excitation has been studied by many researchers. For example, Veletsos and Newmark [30] showed that for a long-period SDOF system, when its natural period $T_n \to \infty$, $u_m/u_0 \to 1$ and $R_y \to \mu$ (equal deformation rule), and that for the response amplitudes governed mainly by the peak excitation velocities, $u_m/u_0 \to \mu/(2\mu-1)^{1/2}$ and $R_y \to (2\mu-1)^{1/2}$ (equal strain energy rule), and for a very high-frequency (stiff) system when $T_n \to 0$, $R_y \to 1$. With a gradual increase in the number of the recorded strong-motion accelerograms [31], the researchers improved these rules to reflect the trends observed in the responses to the recorded data [32–35], for different site conditions and ductility factors [36,37], for rupture distance and the earthquake magnitude [38], and for fault-normal near-field records in the zone affected by directivity [39,40]. Ruiz-Garcia and Miranda [41] noted that the average value of the ratio u_m/u_0 is not much influenced by the recording site classification, by earthquake magnitude, when u_0/u, <4, or by rupture distance. Tiwari and Gupta [42] and Chakraborti and Gupta [43] presented comprehensive regression models based on large data sets and showed clear dependence of the strength-reduction factors on magnitude, predominant period, duration of strong motion, and geologic site conditions. Jalali and Trifunac [44] found strong dependence of R_y versus T_n on the magnitude of an earthquake near the faults. They showed that the classical design curves are conservative for fault-normal pulses, although for fault-parallel displacement the common design rules are not conservative. They recommended that for design close to active faults, the strength-reduction factors for all components of synchronous motion should be constant for all periods and equal to $(2\mu-1)^{1/2}$.

The purposes of this paper are (1) to show how the wave-passage effects influence the strength-reduction factors of the structure subjected to near-fault pulses and displacements and (2) to evaluate the reliability of the classical design curves in such environment.

2. The model

The nature of relative motion of individual column foundations or of the entire foundation system will depend upon the type of foundation and stiffness of the connecting beams and slabs, the characteristics of the soil surrounding the foundation, the type of incident waves, and the direction of wave arrival. In reality, at the base of each column the motion has six degrees of freedom. For simplicity, we consider only the horizontal component of relative motion

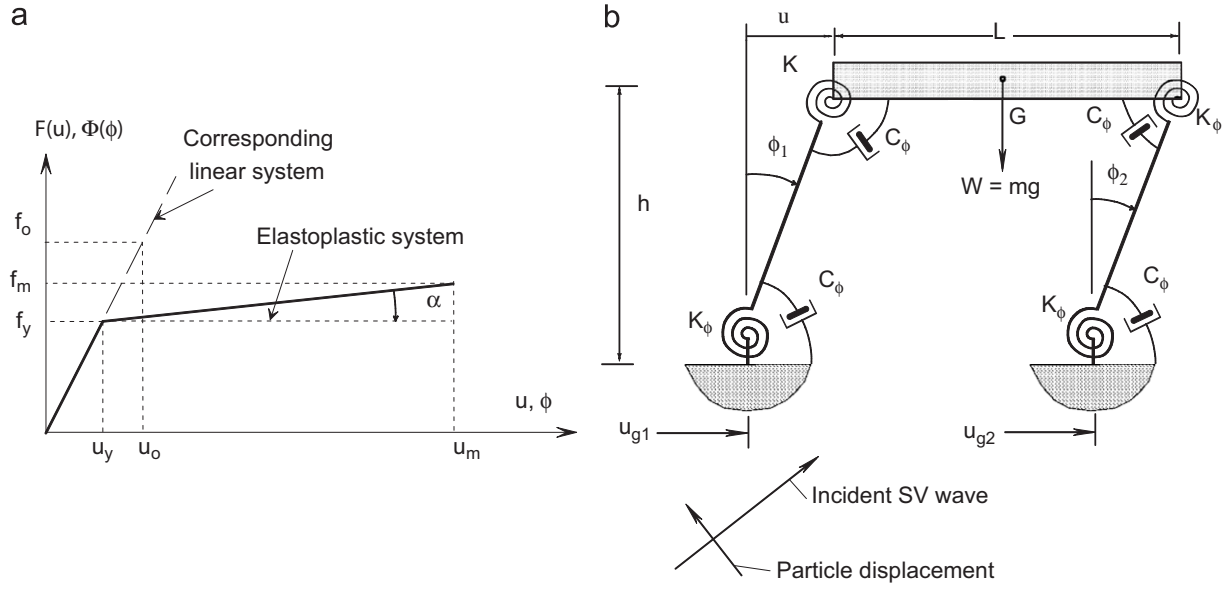

Fig. 1. Left (a): Force-displacement (moment-rotation) relationship for bi-linear spring. Right (b): Relative responses of the system excited by differential ground motions, u_{g1}, u_{g2}. Excitation is illustrated for vertically polarized shear wave (SV).

of column foundations. In this paper, analysis will be performed for structures on isolated foundations only. We assume that the structure is near the fault and that the longitudinal axis of the structure (X-axis) coincides with the radial direction (r-axis) of the propagation of waves from the earthquake source so that the absolute displacement of the base of columns are different, as a result of the wave passage. We suppose that the excitations at piers have the same amplitude with different phase. The phase difference or time delay depends upon the distance between piers and the horizontal phase velocity of the incident waves. The model we consider is shown in Fig. 1b. It represents a one-story structure consisting of a rigid mass, m, with length L, supported by two rigid mass-less columns with height h, which are connected at the top to the mass by rotational springs and at the bottom by rotational springs to the ground. The stiffness of the springs, k_ϕ, is assumed to be elastic–plastic, as shown in Fig. 1a, without hardening ($\alpha = 0$). The mass-less columns are connected to ground and to the rigid mass by circular dashpots, c_ϕ, providing the fraction of critical damping equal to 5 percent. Rotation of the columns, ϕ_i, $i = 1, 2$, which is assumed not to be small, leads us to consider the geometric non-linearity. The mass is acted upon by the acceleration of gravity, g, and is excited by differential horizontal ground motions, u_{g_i}, $i = 1, 2$, at two bases so that $u_{g_2}(t) = u_{g_1}(t-\tau)$ with τ being the time delay between two ground motions. The functional form of u_{g_i} is defined by near-fault ground motions d_F and d_N, which are described in the next section. The governing differential equation for the system in Fig. 1b is then Jalali and Trifunac [44]

$$\left\{A + \frac{(B\cos\phi_1 - C\sin\phi_1)}{(B\cos\phi_2 - C\sin\phi_2)}D\right\}\ddot{\phi}_1(t) + \left\{F - \frac{E}{(B\cos\phi_2 - C\sin\phi_2)}D\right\} = 0,$$

$$(L + u_{g_2} + h\sin\phi_2 - u_{g_1} - h\sin\phi_1)^2 + h^2(\cos\phi_2 - \cos\phi_1)^2 - L^2 = 0, \quad (1)$$

where

$$A = -\frac{1}{2} - \frac{\sin\phi_1\sin(\phi_2-\phi_1)}{6\cos\phi_2},$$

$$B = \frac{L + u_{g_2} - u_{g_1}}{h} + \sin\phi_2 - \sin\phi_1,$$

$$C = \cos\phi_2 - \cos\phi_1,$$

$$D = -\frac{1}{2}\cos(\phi_2-\phi_1) - \frac{\sin\phi_2\sin(\phi_2-\phi_1)}{3\cos\phi_2},$$

$$E = \left(\frac{\dot{u}_{g_2} - \dot{u}_{g_1}}{h} - \cos\phi_1\dot{\phi}_1 + \cos\phi_2\dot{\phi}_2\right)^2 + \left(\sin\phi_1\dot{\phi}_1 - \sin\phi_2\dot{\phi}_2\right)^2 + B\left(\frac{\ddot{u}_{g_2} - \ddot{u}_{g_1}}{h} + \sin\phi_1\dot{\phi}_1^2 - \sin\phi_2\dot{\phi}_2^2\right) + C\left(\cos\phi_1\dot{\phi}_1^2 - \cos\phi_2\dot{\phi}_2^2\right),$$

$$F = -\frac{1}{2}\cos\phi_1\left(\frac{\ddot{u}_{g_2} + \ddot{u}_{g_1}}{h} - \sin\phi_1\dot{\phi}_1^2 - \sin\phi_2\dot{\phi}_2^2\right) + \left(\frac{g}{h} - \frac{1}{2}\left(\cos\phi_1\dot{\phi}_1^2 + \cos\phi_2\dot{\phi}_2^2\right)\right) \times \left(\sin\phi_1 + \frac{\sin(\phi_2-\phi_1)}{2\cos\phi_2}\right) - \frac{1}{12}\left(\cos\phi_2\dot{\phi}_2^2 - \cos\phi_1\dot{\phi}_1^2\right)\frac{\sin(\phi_2-\phi_1)}{\cos\phi_2} + M_1\left(\frac{h\sin(\phi_2-\phi_1)}{L\cos\phi_2} - 2\right) + M_2\left(\frac{h\sin(\phi_2-\phi_1)}{L\cos\phi_2} - \frac{2\cos\phi_1}{\cos\phi_2}\right),$$

$$M_1 = \frac{\omega_n^2}{4}\Phi(\phi_1) + \frac{1}{2}\varsigma\omega_n\dot{\phi}_1,$$

$$M_2 = \frac{\omega_n^2}{4}\Phi(\phi_2) + \frac{1}{2}\varsigma\omega_n\dot{\phi}_2,$$

$$u_{g_2}(t) = u_{g_1}(t-\tau),$$

$$\tau = \frac{L}{C_x}, \quad (2)$$

where C_x is the horizontal phase velocity of incident waves; ω_n and ς are the circular natural frequency and damping ratio of the system, respectively, and $\Phi(\phi)$ is a non-linear function of the type described in Fig. 1a.

3. Near-field ground motion

In general, it is not possible to predict the detailed nature of the near-fault ground motion and of the associated pulses due to irregular distribution of fault slip and because of non-uniform distribution of geologic rigidities surrounding the fault, non-uniform distribution of stress on the fault, and complex non-linear processes that accompany the faulting (e.g., [45–47]). So, in this paper, we adopt a simplified approach and model these motions by smooth pulses, which have correct average amplitudes and duration, and which have been compared to and calibrated against the observed fault slip and the recorded strong motions in terms of their peak amplitudes in time and their spectral content [48,49].

Fig. 2 shows schematically a fault and two characteristic simple motions, d_N and d_F, which describe fault-parallel displacement and fault-normal pulse, respectively. For excitation by a pulse, we chose the Brune's pulse (Fig. 2-center)

$$d_F(t) = A_F t\, e^{-\alpha_F t}, \quad (3)$$

where the typical values of A_F and α_F, for different earthquake magnitudes, are shown in Table 1 [48]. Since the strong-motion data are abundant only up to about $M = 6.5$, we place the values of α_F and A_F, for $M = 7$ and 8, in Tables 1 and 2 in parentheses to emphasize that those are based on extrapolation. For the near-field permanent displacement, we consider the Brune's displacement (Fig. 2 (bottom))

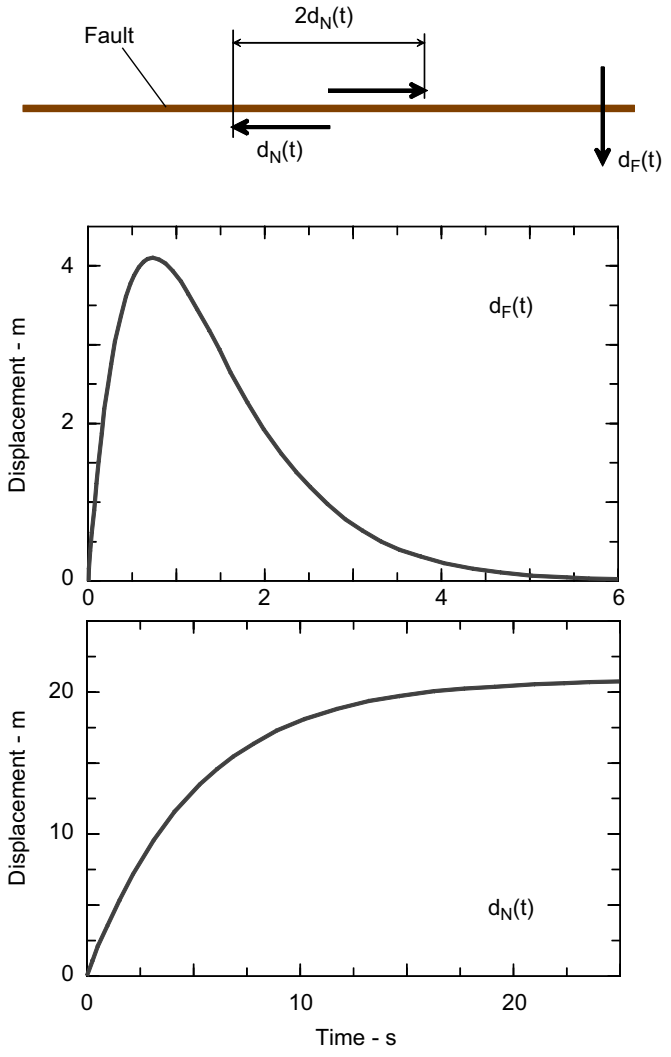

Fig. 2. Fault parallel, $d_N(t)$, and fault-normal, $d_F(t)$, displacements.

Table 1
Characteristics of Brune's pulse displacement [48]

M (magnitude)	σ_F (1/s)	A_F (cm/s)	$d_{F,\max}$ (cm)	$\dot{d}_{F,\max}$ (cm/s)
4	14.04	56.48	1.48	56.48
5	7.90	151.61	7.06	151.61
6	4.44	546.97	45.32	546.97
7	(2.50)	(860.34)	(126.6)	(860.34)
8	(1.40)	(1560.29)	(410.0)	(1560.29)

() Extrapolations based on presently available strong motion data.

$$d_N(t) = \frac{A_N}{2}(1 - e^{-t/\tau_N}). \quad (4)$$

The values of A_N and τ_N, for different earthquake magnitudes, are shown in Table 2 [48].

Mavroeidis et al. [45] have shown that the impulsive near-field strong motion can be approximated by long-period velocity pulses, which are modeled by a modulated cosine function, and have predominant period (duration)

Table 2
Characteristics of Brune's near-fault displacement [48]

M (magnitude)	τ_N (s)	A_N (cm)	$d_{N,\max}$ (cm)	$\dot{d}_{N,\max}$ (cm/s)
4	0.55	4.9	2.45	4.45
5	1.2	29.2	14.6	12.17
6	1.8	245.5	122.75	68.19
7	(3.0)	(1288.0)	(644.0)	(214.7)
8	(5.0)	(4169.0)	(2084.5)	(416.9)

() Extrapolations based on presently available strong motion data.

T_p. They approximated $\log T_p$ by a straight line versus moment magnitude, through nine estimates of barrier intervals previously determined in the source mechanism studies by Papageorgiou and Aki [50]. They noted that in their studies of response, T_p emerges as a key parameter governing the nature of relative linear and non-linear responses, and recommended that all representations of spectral amplitudes, and of the strength-reduction factors should be presented versus T_n/T_p, where T_n is the natural period of SDOF system. The nature of their modulated cosine pulses is such that the velocity gradually starts from zero. In contrast, the broad-band near-fault displacements d_F and d_N, as defined above, are characterized by large initial velocities (Fig. 2), which are proportional to the stress drop in the Brune's ω^2 source model [48]. As has been shown in Jalali and Trifunac [44], this large initial velocity is the key variable in our studies of the role of near-source motions on the response of structures, and for determination of the strength-reduction factors to be used with this response.

4. Strength-reduction factor for columns under differential ground motions

The yield strength-reduction factor for the system under synchronous ground motion is $R_y = f_0/f_y = u_0/u_y$, where all the quantities are defined as in Fig. 1a. In this paper, because of the differential motions of the ground at two piers, the relative rotation of the two columns will be different, and therefore, the ductility demand for these two columns will also be different. So, it is necessary to define the ductility and R factors for each column instead of one factor for the total system. For the ith column we have

$$R_{y_i} = \frac{\Phi_{0_i}}{\Phi_y} = \frac{\phi_{0_i}}{\phi_y},$$
$$\mu_i = \frac{\phi_{m_i}}{\phi_y}. \quad (5)$$

Φ_{0_i}, ϕ_{0_i}, and ϕ_{m_i} are the maximum linear moment, linear rotation, and non-linear rotation of ith column, respectively. Φ_y and ϕ_y are the yield moment and rotation of columns, respectively. For ductility μ_i, the inelastic deformation ratio ϕ_{m_i}/ϕ_{0_i} is then equal to μ_i/R_{y_i}. The inelastic deformation ratio for known yield strength and

excitation $C_{R_{y_i}} = \phi_{m_i}/\phi_{0_i} = \mu_i/R_{y_i}$ can be computed from calculated peak responses ϕ_{m_i} and ϕ_{0_i}. For given R_{y_i}, the associated ductility demand is then determined from μ_i/R_{y_i}. Iterations are required to compute the inelastic deformation ratio, $C_{\mu_i} = \phi_{m_i}/\phi_{0_i}$ for a specified ductility factor because different values of Φ_y may lead to the same μ_i. Because C_{μ_i} is not unique, the convention is to choose the largest Φ_y corresponding to the largest C_{μ_i} [51].

5. Response of the system subjected to near-fault differential ground motions d_F and d_N

In all calculations, we consider simultaneous action of the effects of gravity forces [52], dynamic instability [53,54], and geometric non-linearity. For this structure, we calculate ϕ_{m_i} and ϕ_{0_i} for the two columns of the system under near-fault differential ground motions d_F and d_N corresponding to earthquake magnitudes $M = 5$, 6, 7, and 8, for ductilities $\mu = 2$, 4, and 8, and for different time delays, $\tau = 0.001$, 0.01, 0.03, 0.05, and 0.1 s, and then plot R_y versus T_n for the two columns. At first, we describe the effect of differential ground motion on the linear response of the system excited by fault-normal pulse and fault-parallel displacement at the fault. Figs. 3a and b show the linear pseudo-relative velocity (PSV) spectra computed for differential ground motions represented by d_F (Fig. 3a) and d_N (Fig. 3b), for magnitudes $M = 4$, 6, 8, and for different time delays, $\tau = 0.001$, 0.01, 0.05, and 0.1 s. The fraction of critical damping is $\varsigma = 0.05$. As we know, for differential ground motions the linear response of the system has two components, dynamic and pseudo-static. For a long-period system, the dynamic component of the response is dominant, and the pseudo-static component is usually small, while for a high-frequency system the response is dominated by the pseudo-static component and the dynamic component is negligible [25,26]. As would be expected, it can be seen from Figs. 3a and b that the effect of differential ground motions is significant for a high-frequency (stiff) system and is negligible for a long-period (flexible) system. When the time delay is small ($\tau = 0.001$), the pseudo-static component of the response is small, and the PSV amplitudes of two columns are approximately the same. In this condition, and for a high-frequency system, the response is dominated by the initial velocity of the ground, $\dot{d}_F$ and $\dot{d}_N$ [44] . For long periods, the response is dominated by the maximum displacement of the ground, $d_{F\max}$ and $d_{N\max}$. With increasing time delay, the contribution of the pseudo-static component becomes larger and the PSV amplitudes of the two columns become different. In this condition, and in a high-frequency range, the PSV amplitudes increase significantly. As can be seen, the PSV amplitudes of the two columns cross each other at the points where the period of the system is approximately equal to $T_n = \tau$, 2τ. At these periods, the system is subjected to in-phase or out-of-phase motions at the two piers.

Fig. 4 illustrates the typical changes of R_y versus the oscillator period for near-fault fault-parallel displacement,

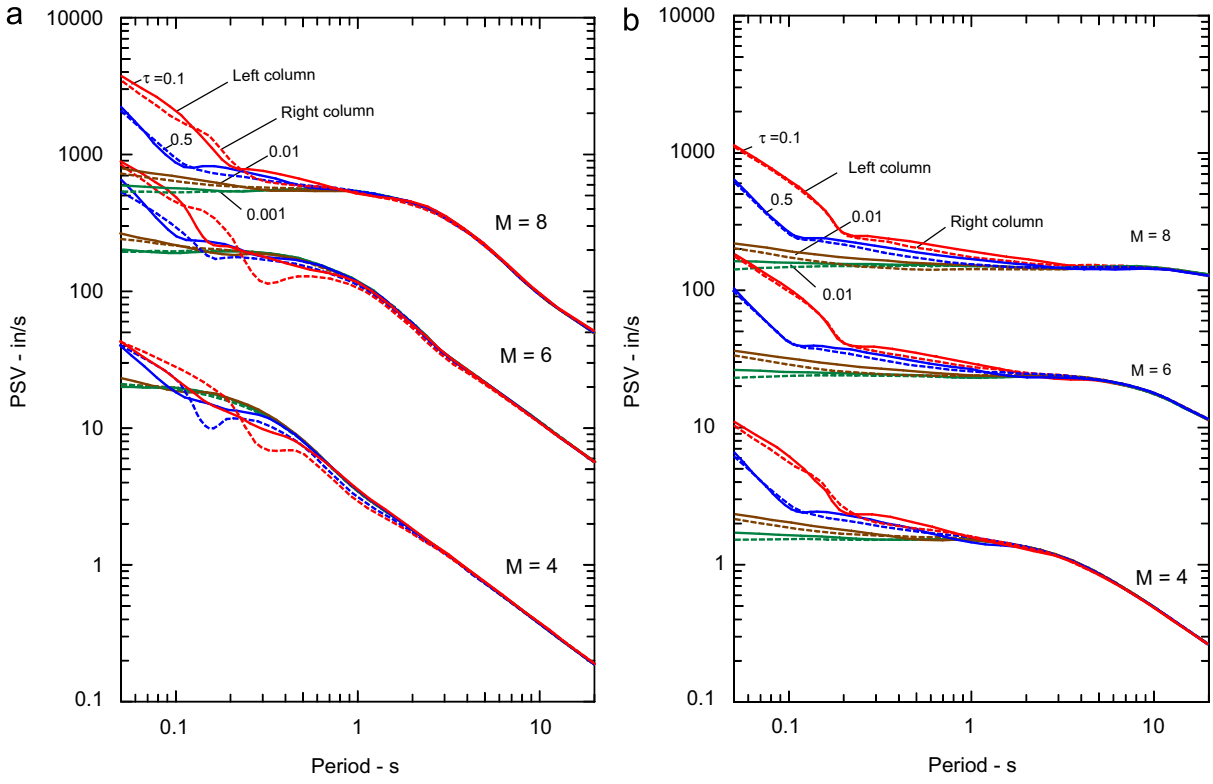

Fig. 3. (a) Influence of the wave-passage effect on PSV spectra for the pulse at the fault, $d_F(t)$ and (b) same as (a), but for excitation by the fault-parallel displacement, $d_N(t)$.

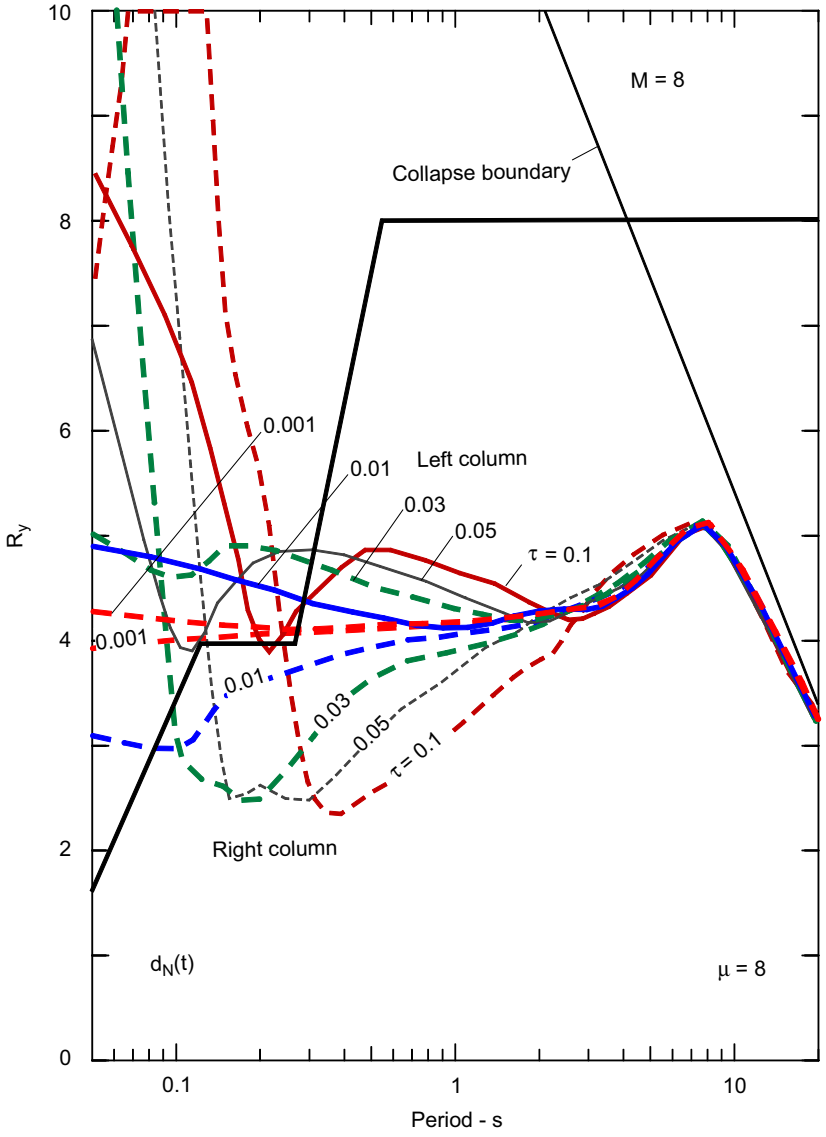

Fig. 4. The effects of time delay on the strength-reduction factors computed for near-fault displacement, $d_N(t)$, for $M = 8$, $\varsigma = 0.05$, and $\mu = 8$, with piecewise straight (continuous line) representation of R_y used in design (redrawn from Chopra, 1996). Ten different continuous and dashed lines show variations in the strength-reduction factors for left and right columns, and for five delay times $\tau = 0.001$, 0.01, 0.03, 0.05, and 0.1.

$M = 8$, for a ductility ratio of eight and for the left and the right columns, assuming wave propagation from left to right in Fig. 1b, and for $\tau = 0.001$, 0.01, 0.03, 0.05, and 0.1 s. For reference and easier comparison among different figures in this paper, and considering the previously published results, we also plotted one of the oldest estimates of R_y versus period [44,55], by piecewise straight lines.

Figs. 5a,b and 6a,b show the strength-reduction factors versus the period of the system under differential ground motions represented by a fault-normal pulse (Figs. 5a and b) and fault-parallel displacement (Figs. 6a and b). For comparison, we again superimposed the classical design curves [55]. As can be seen from these figures, the wave-passage effects on the strength-reduction factor are significant for a high-frequency system and negligible for a flexible system. For long periods (displacement-sensitive region), the R factors of the two columns are nearly the same and tend to asymptotic values equal to μ or the values for which collapse occurs because of the destabilizing effect of gravity. For the parameters considered in this paper, these collapse boundaries appear for $T_n < 20$ s, for $\mu \geqslant 4$, and for $M > 7$, for excitation by d_F (Fig. 5b), and for $\mu \geqslant 4$ and $M > 5$ for excitation by d_N (Fig. 6a,b). The values of R_y for which collapse occurs are shown by almost straight lines with negative slopes, asymptotically approaching R-curves from above.

For very high frequencies and for a small time delay $\tau = 0.001$, the strength-reduction factors of the system tend to an asymptote with amplitude equal to $(2\mu - 1)^{1/2}$ (same as the first horizontal plateau of simplified R_y curves), the consequence of strong initial velocity associated with a sudden onset of near-fault ground motions [44]. With increasing the time delay and for a stiff system, relative

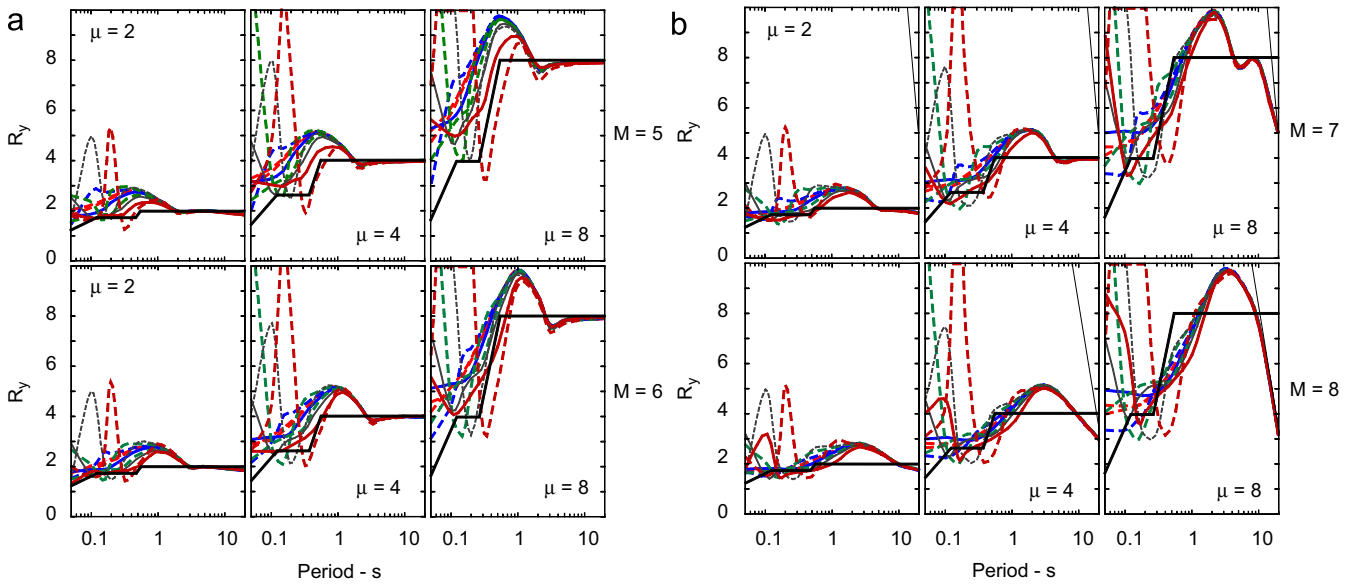

Fig. 5. (a) The effects of time delay on the strength-reduction factors computed for fault-normal pulse, $d_F(t)$, for $M = 5$ and 6, $\varsigma = 0.05$, and $\mu = 2$, 4, 8, with piecewise straight (continuous line) representation of R_y used in design (redrawn from Chopra, 1996). Ten different continuous and dashed lines show variations in the strength-reduction factors for left and right columns, and for five delay times $\tau = 0.001$, 0.01, 0.03, 0.05, and 0.1. Presentation of these lines (weight, continuous, dashed) is identical to those shown in Fig. 4. (b) Same as (a), but for $M = 7$, 8.

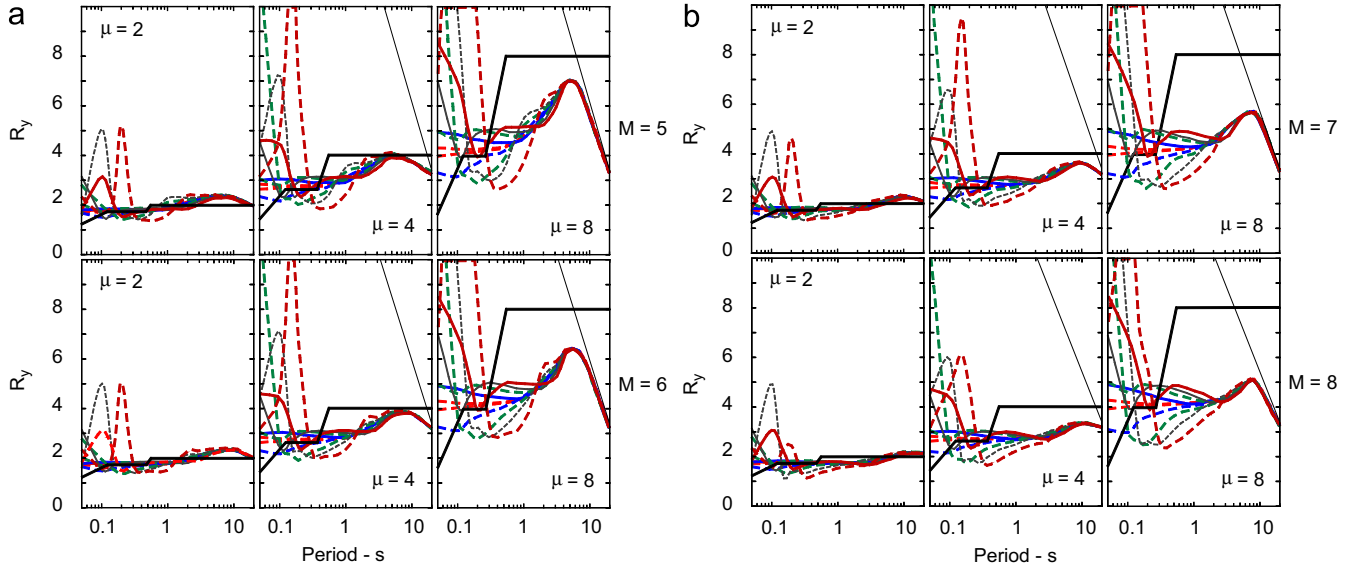

Fig. 6. (a) The effects of time delay on the strength reduction factors computed for fault-parallel displacement, $d_N(t)$, for $M = 5$ and 6, $\varsigma = 0.05$, and $\mu = 2$, 4, 8, with piecewise straight (continuous line) representation of R_y used in design (redrawn from Chopra, 1996). Ten different continuous and dashed lines show variations in the strength-reduction factors for left and right columns, and for five delay times $\tau = 0.001$, 0.01, 0.03, 0.05, and 0.1. Presentation of these lines (weight, continuous, dashed) is identical to those shown in Fig. 4. (b) Same as (a), but for $M = 7$, 8.

rotations of the two columns are not the same. In other words, for each value of ductility, the R factors of two columns are completely different, and their difference depends upon the time delay, magnitude of the earthquake, and the period of the system. For very high frequency, the R-factor of the two columns could be smaller or larger than $(2\mu-1)^{1/2}$. From Figs. 5a and b, it can be seen that for magnitude $M = 5$ and for different time delays, our result is above the classical strength-reduction factor, except for $\tau = 0.1$ s, and for a short interval in T_n ($0.3\,\text{s} < T_n < 0.8\,\text{s}$). For magnitude $M = 6$, 7, and 8, and for $\tau = 0.03$, 0.05, 0.1, the classical design curves are not conservative for periods between about 0.1 and 1.0 s. In Figs. 6a and b and for near-fault displacement d_N, when the time delay is small, $\tau = 0.001$, for a high-frequency system (T_n shorter than about 0.2–0.4 s), the classical design curves are conserva-

tive, but with increasing time delay, the R-factor of the columns is under the classical design curves for essentially all periods.

6. Conclusions

We have illustrated the wave-passage effects on the strength-reduction factor, R_y versus T_n, for a simple two-column system subjected to near-fault ground motions. Our results show that the effect of differential ground motion is significant for linear and non-linear response of a high-frequency system, while the wave-passage effect is negligible for a long-period system. When the time delay is short, and for a stiff system, the PSV amplitude and R-factor of the two columns are approximately the same and are dominated by the initial velocity of the ground motion [44] . In this case, the PSV amplitude tends to initial velocity of the ground, $\dot{d}_{\mathrm{F}}$ and $\dot{d}_{\mathrm{N}}$, and the R-factor amplitude tends to $(2\mu-1)^{1/2}$. By increasing the time delay, and for a stiff system, because of the pseudo-static component of the response, the PSV amplitudes for the columns increase and the R factors of the two columns are completely different.

For small values of time delay and for pulse-like fault-normal motions near fault, which we modeled in this paper by d_{F}, our calculation is above the classical design curves. However, with increasing the time delay the classical design curves are not conservative for periods between about 0.1 and 1.0 s.

For fault-parallel motions modeled in this paper by d_{N}, and for all time delays, our calculations give R factors smaller than the classical R values. With increasing time delay, the R factors move down, and for essentially all periods the classical design curves are not conservative.

Acknowledgments

We are indebted to anonymous reviewers whose valuable comments and suggestions led to significant improvements in the text, and to better presentation of the figures.

References

[1] Bogdanoff JL, Goldberg JE, Schiff AJ. The effect of ground transmission time on the reponse of long structures. Bull Seism Soc Am 1965;55:627–40.
[2] Harichandran RS, Vanmarcke EH. Stochastic variation of earthquake ground motion in space and time. J Eng Mech Div ASCE 1986;112(2):154–74.
[3] Hao H. Effects of spatial variations of ground motion on large multiply-supported structures. Report no. EERC 89-06, Earthquake England Research Laboratory, University of California at Berkeley, Berkeley, CA, 1989.
[4] Loh CH, Penzien J, Tsai YB. Engineering analysis of SMART-1 array accelerograms. Earthquake Eng Struct Dyn 1982;10:575–91.
[5] Harichandran RS, Wang W. Response of simple beam to spatially varying earthquake excitation. J Eng Mech Div ASCE 1988;114: 1526–41.
[6] Harichandran RS, Wang W. Response of intermediate two-span beam to spatially varying seismic excitation. Earthquake Eng Struct Dyn 1990;19:173–87.
[7] Zerva A. Effect of spatial variability and propagation of seismic ground motions on the response of multiply supported structures. Prob Eng Mech 1991;6:212–21.
[8] Hyun CH, Yun CB, Lee DG. Non-stationary response analysis of suspension bridges for multiple support excitations. Prob Eng Mech 1992;7(1):27–35.
[9] Kashefi I, Trifunac MD. Investigation of earthquake response of simple bridge structures. Report no. CE 86-02, Department of Civil Engineering, University of Southern California, Los Angeles, CA, 1986.
[10] Perotti F. Structural response to non-stationary multiple support random excitation. Earthquake Eng Struct Dyn 1990;19:513–27.
[11] Hao H. Response of multiply supported rigid plate to spatially correlated seismic excitation. Earthquake Eng Struct Dyn 1991; 20:821–38.
[12] Todorovska MI, Lee VW. Seismic waves in buildings with shear walls or central core. J Eng Mech Div ASCE 1989;115(12):2669–86.
[13] Todorovska MI, Trifunac MD. Antiplane earthquake waves in long structures. J Eng Mech Div ASCE 1989;115(12):2687–708.
[14] Todorovska M I, Trifunac MD. A note on the propagation of earthquake waves in buildings with soft first floor. J Eng Mech Div ASCE 1990;116(4):892–900.
[15] Todorovska MI, Trifunac MD. A note on excitation of long structures by ground waves. J Eng Mech Div ASCE 1990; 116(4):952–64.
[16] Kojic S, Trifunac MD. Earthquake response of arch dams to non-uniform canyon motion. Report no. CE 88-03, Department of Civil England, University of Southern California, Los Angeles, CA, 1988.
[17] Kojic S, Trifunac MD. Earthquake stresses in arch dams: I—theory and antiplane excitation. J Eng Mech Div ASCE 1991;117(3):532–52.
[18] Kojic S, Trifunac MD. Earthquake stresses in arch dams: II—excitation by SV, P and Rayleigh waves. J Eng Mech Div ASCE 1991;117(3):553–74.
[19] Berrah M, Kausel E. Modified response spectrum model for the design of structures subjected to spatially varying seismic excitations. MIT research report R90-2, Massachusetts Institute of Technology, Cambridge, MA, 1990.
[20] Betti R, Panariello GF. Active control of structures subjected to spatially varying earthquake excitation. In: Proceedings of the first world conference on Structural Control. vol. 2. TP2-79-TP2-88, 1994.
[21] Der-Kiureghian A, Neuenhofer A. Response spectrum method for multisupport seismic excitation. Earthquake Eng Struct Dyn 1992;21:713–40.
[22] Okubo T, Arakawa T, Kawashima T. Preliminary analysis of finite ground strains induced during earthquake and effect of spatial ground motions on structural response. In: International symposium on lifeline earthquake engineering, fourth US national conference on pressure vessels and piping technology. ASME, Portland, Oregon, 1983.
[23] Zembaty Z, Krenk S. Spatial seismic excitations and response spectra. J Eng Mech Div ASCE 1993;119:2449–59.
[24] Zembaty Z, Krenk S. Reponse spectra of spatial seismic ground motion. In: 10th European Conference on earthquake engineering. vol. 2. Vienna, Austria, 1271–5, 1994.
[25] Trifunac MD, Gicev V. Response spectra for differential motion of columns, paper II: out-of-plane response. Soil Dyn Earthquake Eng 2006;26(12):1149–60.
[26] Trifunac MD, Todorovska MI. Response spectra and differential motion of columns. Earthquake Eng Struct Dyn 1997;26(2):251–68.
[27] Applied Technology Council (ATC). Seismic evaluation and retrofit of concrete buildings. Report no ATC-40, Redwood City, CA, 1996.
[28] Federal Emergency Management Agency (FEMA). NEHRP guidelines for the seismic rehabilitation of buildings. Report no. FEMA-273 (guidelines) and report no. FEMA-274 (commentary), Washington, DC, 1997.

[29] Federal Emergency Management Agency (FEMA). Prestandard and commentary for seismic rehabilitation of buildings. Report no. FEMA-356, Washington, DC, 2000.
[30] Veletsos AS, Newmark NM. Effect of inelastic behavior on the response of simple systems to earthquake motions. In: Proceedings of the second world conference on earthquake engineering. vol. II, 1960. p. 859–912.
[31] Trifunac MD, Todorovska MI. Evolution of accelerographs, data processing, strong motion arrays and amplitude and spatial resolution in recording strong earthquake motion. Soil Dyn Earthquake Eng 2001;21(6):537–55.
[32] Chopra AK, Chintanapakdee C. Comparing response of SDOF systems to near-fault motions in the context of spectral regions. Earthquake Eng Struct Dyn 2001;30(12):1769–89.
[33] Riddell R, Garcia J, Garces E. Inelastic deformation response of SDOF systems subjected to earthquakes. Earthquake Eng Struct Dyn 2002;31(3):515–38.
[34] Veletsos AS, Vann WP. Response of ground-excited elastoplastic systems. J Struct Div ASCE 1971;97(4):1257–81.
[35] Veletsos AS, Newmark NM, Celapati CV. Deformation spectra for elastic and elastoplastic systems subjected to ground shock and earthquake motion. In: Proceedings of the third world conference on earthquake engineering. vol. II, p. 663–82, Wellington, New Zealand, 1965.
[36] Miranda E. Seismic evaluation and upgrading of existing structures. PhD thesis, University of California at Berkeley, Berkeley, CA, 1991.
[37] Ruiz-Garcia J, Miranda E. Inelastic displacement ratios for evaluation of structures built on soft soil sites. Earthquake Eng Struct Dyn 2006;35(6):679–94.
[38] Miranda E. Inelastic displacement ratios for structures on firm sites. J Struct Eng 2000;126(10):1150–9.
[39] Baez JI, Miranda E. Amplification factors to estimate inelastic displacement demands for the design of structures in the near field. In: Proceedings of the 12th world conference on earthquake engineering (CD-ROM). Auckland, New Zealand, 2000.
[40] MacRae GA, Morrow DV, Roeder CW. Near-fault ground motion effects on simple structures. J Struct Eng 2001;127(9):996–1004.
[41] Ruiz-Garcia J, Miranda E. Inelastic displacement ratios for evaluation of existing structures. Earthquake Eng Struct Dyn 2003; 32(8):1237–58.
[42] Tiwari AK, Gupta VK. Scaling of ductility and damage-based strength reduction factors for horizontal motions. Earthquake EngStruct Dyn 2000;29(7):969–87.
[43] Chakraborti A, Gupta VK. Scaling of strength reduction factors for degrading elasto-plastic oscillators. Earthquake Eng Struct Dyn 2005;34(2):189–206.
[44] Jalali RS, Trifunac MD. A note on strength reduction factors for design of structures near earthquake faults, 2007, submitted for publication.
[45] Mavroeidis GP, Dong G, Papageorgiou AS. Near-fault ground motions, and the response of elastic and inelastic single-degree-of-freedom (SDOF) systems. Earthquake Eng Struct Dyn 2004;33(9): 1023–49.
[46] Trifunac MD. A three-dimensional dislocation model for the San Fernando, California, earthquake of February 9, 1971. Bull Seism Soc Am 1974;64(1):149–72.
[47] Trifunac MD, Udwadia FE. Parkfield, California, earthquake of June 27, 1966: a three-dimensional moving dislocation. Bull Seism Soc Amer 1974;64(3):511–33.
[48] Trifunac MD. Broad-band extension of Fourier amplitude spectra of strong motion acceleration. Report CE 93-01, Department of Civil Engineering University of Southern California, Los Angeles, CA, 1993.
[49] Trifunac MD, Todorovska MI. Broad-band extension of pseudo-relative velocity spectra of strong motion, Report CE 94-02, Department of Civil Engineering University of Southern California, Los Angeles, CA, 1994.
[50] Papageorgiou AS, Aki K. A specific barrier model for quantitative description of inhomogeneous faulting and the prediction of strong ground motion, I: Description of the model. Bull Seism Soc Am 1983;73(3):693–722.
[51] Veletsos AS, Newmark NM. Response spectra for single-degree-of-freedom elastic and inelastic systems, Report no. RTD-TDR-63-3096, vol. III, Air Force Weapons Laboratory, Albuquerkque, NM, 1964.
[52] Husid R. Gravity effects on the earthquake response of yielding structures. PhD thesis, California Institute of Technology, Pasadena, CA, 1967.
[53] Bolotin VV. The Dynamic Stability of Elastic Systems. San Francisco, California: Holden Day; 1964.
[54] Lee VW. Investigation of Three-Dimensional Soil-Structure Interaction, Department of Civil Engineering, Report CE. 79-11, University of Southern California, Los Angeles, CA; 1979.
[55] Chopra AK. Dynamics of structures: theory and applications to earthquake engineering. New Delhi: Prentice-Hall of India; 1996.